

Towards a Fluctuation Theorem in an Atmospheric Circulation Model

B. Schalge, R. Blender, J. Wouters, K. Fraedrich, and F. Lunkeit

Meteorologisches Institut, KlimaCampus, Universität Hamburg, Hamburg, Germany

(Dated: June 18, 2018)

An investigation of the distribution of finite time trajectory divergence is performed on an Atmospheric Global Circulation Model. The distribution of the largest local Lyapunov exponent shows a significant probability for negative values over time spans up to 10 days. This effect is present for resolutions up to wave numbers $\ell = 42$ ($\approx 250\text{km}$). The probability for a negative local largest Lyapunov exponent decreases over time, similarly to the predictions of the Fluctuation Theorem for entropy production. The model used is hydrostatic with variable numbers of vertical levels and different horizontal resolutions.

PACS numbers: 92.60.Bh, 92.70.Np, 05.70.Ln

I. INTRODUCTION

The fluctuation theorem (FT) [1, 2] describes the probability of negative entropy production in nonlinear nonequilibrium systems. It shows how such a violation of the second law becomes exponentially unlikely when the period over which entropy production is measured increases. This FT has been observed to hold in experiments and numerical simulations of turbulent flows [3, 4].

In atmospheric models, similar processes can be observed. In this case a violation of the second law can be associated with an increase of predictability (return of skill) [5], indicating that for certain flow configurations an error, seen as a finite perturbation to the trajectory, decreases over time.

Studies of fluctuation theorems are often directed at mesoscopic systems, such as molecular motors or proteins, having a moderate number of degrees of freedom. The numerical modelling of continuous systems is restricted to a finite number of degrees of freedom which also has to be moderate if long time spans have to be covered. Therefore, we can expect that deviations from the second law as described by the FT may occur also in such numerical simulations.

In this paper we consider simulations with an atmospheric Global Circulation Model (GCM). Models of this type form the hydrostatic dynamical cores of complex weather and climate models. They simulate the stratified large scale flow on a rotating sphere driven by a temperature relaxation and subject to linear surface friction and hyper-diffusion. The flow is characterised by quasi-two-dimensional turbulence and Rossby waves [6]. By changing horizontal and vertical resolutions of the model the number of degrees of freedom can be modified.

Instead of using the common dynamical system formulation of entropy production as the phase space contraction rate, we choose a simplified approach. The entropy production Σ is identified with the 'entropy-like quantity' (related to the Kolmogorov or metric entropy) k_n [7, 8] defined as the local error growth given by the largest local Lyapunov exponents $\hat{\lambda}$. In the long time limit the $\hat{\lambda}$ tend

to the largest Lyapunov exponent λ_{max} . For a summary on the definitions of entropy in dynamical systems, in particular the relationship with topological entropy see Young [9]. Previously, studies of the distribution of $\hat{\lambda}$ have been performed for simple one-dimensional dynamical systems, showing that these distributions can in certain cases be Gaussian due to a central limit theorem [10], however, in general distinct deviations from Gaussianity are found [11].

In Sections II and III the model and the analysis are described. Section IV includes the results for the statistics of $\hat{\lambda}$ and the validity of the FT, and in Section V we summarize the results and discuss the conclusions.

II. GLOBAL CIRCULATION MODEL

In this paper we utilize the Portable University Model of the Atmosphere (PUMA) [12, 13], a hydrostatic global atmospheric model based on the multi-layer primitive equations on the sphere. Model variables are vorticity, horizontal divergence, temperature and logarithmic surface pressure. The complete equations of PUMA are

$$\partial_t \xi = s^2 \partial_\lambda \mathcal{F}_v - \partial_\mu \mathcal{F}_u - \frac{1}{\tau_f} \zeta - K \nabla^8 \zeta \quad (1)$$

$$\begin{aligned} \partial_t D = s^2 \partial_\lambda \mathcal{F}_u + \partial_\mu \mathcal{F}_v - \nabla^2 \left[\frac{s^2}{2} (U^2 + V^2) \right. \\ \left. + \Phi + \bar{T} \ln p_s \right] - \frac{1}{\tau_f} D - K \nabla^8 D \end{aligned} \quad (2)$$

$$\begin{aligned} \partial_t T' = -s^2 \partial_\lambda (UT') - \partial_\mu (VT') + DT' - \dot{\sigma} \frac{\partial T}{\partial \sigma} \\ + \kappa \frac{T\omega}{p} + \frac{1}{\tau_c} (T_R - T) - K \nabla^8 T' \end{aligned} \quad (3)$$

$$\partial_t \ln p_s = -s^2 U \partial_\lambda \ln p_s - V \partial_\mu \ln p_s - D - \frac{\partial \dot{\sigma}}{\partial \sigma} \quad (4)$$

$$\frac{\partial \Phi}{\partial \ln \sigma} = -T \quad (5)$$

where $\mu = \sin \phi$, $s^2 = 1/(1 - \mu^2)$. ζ and ξ denote absolute and relative vorticity, D is the horizontal di-

vergence and p_s the surface pressure. The temperature T is divided into a background state, \bar{T} , and an anomaly, T' . Spherical coordinates are given by λ and ϕ for longitude and latitude respectively, $s^2 = 1/(1 - \sin^2 \phi)$, Φ is the geopotential, κ is the adiabatic coefficient, ω is vertical velocity and K a diffusion coefficient. We also use the abbreviations $U = u \cos \phi$ and $V = v \cos \phi$ (u, v are the zonal and meridional velocities, resp.), $\mathcal{F}_u = V\zeta - \dot{\sigma}\partial U/\partial\sigma - T'\partial \ln p_s/\partial\lambda$ and $\mathcal{F}_v = -U\zeta - \dot{\sigma}\partial V/\partial\sigma - T's^{-2}\partial \ln p_s/\partial \sin \phi$. The vertical coordinate is divided into equally spaced σ -levels ($\sigma = p/p_s$, where p and p_s denote the pressure and the surface pressure, respectively).

To maintain a stationary state the model is driven by a Newtonian cooling formulation towards a constant temperature profile with an equator-to-pole gradient (i.e., a term $(T_R - T)/\tau_c$ is added to the temperature equation, where τ_c is the time scale, T denotes the actual model temperature and T_R refers to the prescribed reference temperature). Dissipation is given by Rayleigh friction in the boundary layer (i.e., terms $-\zeta/\tau_f$ and $-D/\tau_f$ are added to the equations for vorticity and divergence, where τ_f is the friction time scale). Hyperdiffusion ($\propto \nabla^8$) accounts for subscale processes and numerical stability.

The equations are numerically solved using the spectral transform method [14]: linear terms are evaluated in the spectral domain while nonlinear products are calculated in grid point space. The horizontal resolution is varied between total spherical wave number $\ell = 15$ and 42 (approx. 7.5° and 2.8° on the corresponding grid). The wave numbers are restricted according to the triangular truncation which is denoted as 'T ℓ ' with the total wave number ℓ . The vertical model resolution is between $L = 5$ and 20 vertical levels. The resolutions considered here restrict the numbers of degrees of freedom to values below 10^5 , i.e. to the range of mesoscopic systems.

The model is integrated by a leap-frog method with a time step of 30min (15min for $\ell = 42$ resolution). Orography is not specified and no external variability like annual or daily cycles are imposed.

Due to the neglect of complex parameterizations like convection, the error growth in a dynamical core model corresponds to the long time growth regime in complex weather and climate models which incorporate a rapid error growth caused by small and fast processes [15].

III. ANALYSIS

As a measure for predictability in the model the linear stability is determined by the simulation of two close nonlinear trajectories. One of the simulations is denoted as reference trajectory $x(t)$ while the second is considered as a perturbed trajectory $\tilde{x}(t)$ initialized with weak random deviations in the surface pressure. The distance $\|x(t) - \tilde{x}(t)\|$ between the trajectories is determined using an Euclidean metric for all model variables in grid point

space. Linear instability of the reference trajectory is assessed by maintaining small distances through a regular rescaling of the perturbation after a time span $\tau_0 = 10$ days to the initial distance d_0 (these intervals are denoted as rescaling intervals in the following). To collapse the perturbation onto the most unstable direction the analysis neglects an initial spin up of 10 rescaling intervals in the 200 years trajectories.

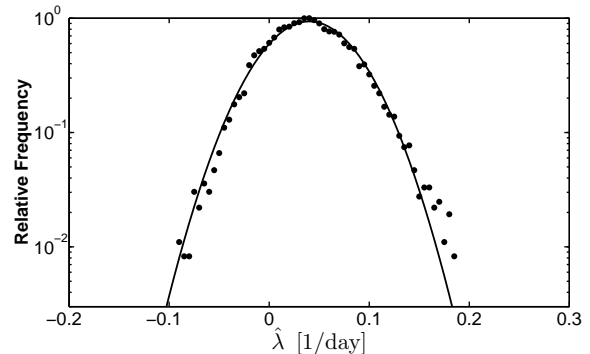


Figure 1. Relative frequencies of the local largest Lyapunov exponent for $\tau = 100$ h with a Gaussian fit (black) for the resolution T21L5.

Within the rescaling intervals of duration τ_0 the growth of the distance d is measured every 5 hours to estimate the local largest Lyapunov exponent $\hat{\lambda}$

$$\hat{\lambda}(t, \tau) = \frac{1}{\tau} \log \frac{d(t, \tau)}{d_0} \quad (6)$$

Here $d(t, \tau) = \|x(t + \tau) - \tilde{x}(t + \tau)\|$, where $t = n\tau_0$ measures the absolute time and $\tau < \tau_0$ is the time elapsed after the last rescaling to the initial distance d_0 . The unit for $\hat{\lambda}$ is $1/day$. In the following the times t characterize the rescaling intervals while τ are the growth times within these intervals.

According to [7, 8] we assess the entropy production Σ by the largest local Lyapunov exponents. Periods with $\hat{\lambda} < 0$ are associated with a return of skill in predictability experiment [16]. As the largest exponent is negative, phase space contracts during these intervals, hence the entropy production is negative.

IV. RESULTS

The distribution of $\hat{\lambda}$ is analysed for a standard low resolution version and for variable vertical and horizontal resolutions. It is demonstrated that an approximation of the entropy production behaves similarly to the predictions of the Fluctuation Theorem. This relation holds for a range of $\hat{\lambda}$ for a fixed growth time τ in a low resolution experiment.

In the standard low resolution version T21L5 of the model (total wave number 21 and 5 vertical levels) 7744

degrees of freedom are present. Due to the numerical efficiency this resolution is frequently used in long-term simulations since it produces a circulation with the characteristic properties of the observations (for example Hadley and Ferrel cells and mid-latitude storms [17]). The exponents are determined for a fixed growth time $\tau = 100$ hours in all sampling intervals ($\tau_0 = 10$ days). Figure 1 shows the distribution of the $\hat{\lambda}$ values with a Gaussian fit (normalized to the maximum). The Gaussian fits in Figure 1 and the following figures are used to characterise the $\hat{\lambda}$ distribution by their means and variances. Deviations from Gaussianity cannot be assessed due to the limited data sets. About 17% of the exponents $\hat{\lambda}$ are negative, hence the model is in a state of negative entropy production for a considerable amount of time.

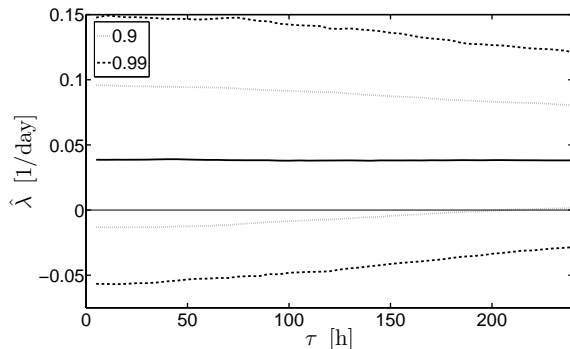


Figure 2. Quantiles (0.9, 0.99) of the local largest Lyapunov exponent. The median (solid) corresponds to the global largest Lyapunov exponent

To characterize the distribution for a wide range of growth times τ the 0.9 and 0.99-quantiles are presented (Figure 2). The growth times τ range from the minimum of 5 hours to the maximum given by the rescaling time $\tau_0 = 10$ days. Thus Figure 1 corresponds to the $\tau = 100$ hours slice in Figure 2. The median is the largest Lyapunov exponent which is by definition independent of the growth time τ . For increasing τ the quantiles approach the median indicating a narrowing distribution. For large τ negative values become less likely and the probability of negative entropy production vanishes.

The sensitivity of the $\hat{\lambda}$ distribution to the vertical model resolution is determined for fixed horizontal resolution T21 (Figure 3) with numbers of levels ranging from 3, 5, 10, to 20. The number of degrees of freedom depends linearly on the number of levels: 4840, 7744, 15004, 29524. Here Gaussian fits to the distributions are shown which are normalized by the maximum (compare Figure 1). All curves show a comparable mean but become broader for increasing numbers of levels. Beyond 10 levels a limit is reached.

For increasing horizontal resolutions and keeping the number of five levels fixed the $\hat{\lambda}$ distributions change differently (Figure 4). The degrees of freedom for five levels are 4096 (T15), 7744 (T21), 16384 (T31) and 28224

(T42).

From T15 to T21 the distribution shifts to more positive means and becomes broader. Similarly to the analysis for the vertical resolution (Figure 3), an increase in the number of degrees of freedom seems to imply an increase in standard deviation.

From T21 to T31 and T31 to T42 the main change is a shift to positive values while the variance increase is negligible (in contrast to Figure 3). Therefore, the frequency of negative $\hat{\lambda}$ decreases with increasing horizontal resolution.

The increase of the horizontal resolution enhances the effective number of degrees of freedom by the simulation of smaller structures like mid-latitude vortices. In contrast, the increase of the vertical resolution beyond 10 levels seems not to yield additional effective degrees of freedom for the given horizontal T21 resolution.

Motivated by the FT, we further analyze the frequency of negative $\hat{\lambda}$ events. The FT relates the ratio of positive to negative entropy production rates Σ with the mean entropy production rate $\bar{\Sigma}$ and the growth time τ for sufficiently large τ

$$\frac{P(\Sigma = +a)}{P(\Sigma = -a)} = e^{a\tau\bar{\Sigma}} \quad (7)$$

To validate this relation, we plot the logarithm of $P(\hat{\lambda} = a)/P(\hat{\lambda} = -a)$, the ratio of the probabilities of observing $\hat{\lambda}$ with values a and $-a$. Figure 5 shows this ratio for different growth times between $\tau = 10$ h and $\tau = 240$ h as well as the slopes of the logarithmic probability ratios. These logarithmic ratios are clear linear functions of Σ . Note that (7) follows for fixed growth time τ when the fluctuations are Gaussian. The slopes of the logarithmic probability ratios increase linearly with growth time τ for $\tau > 160$ h as indicated by the relation (7). For finite times there is a non-negligible probability for negative entropy production rates, which vanishes in the long time limit.

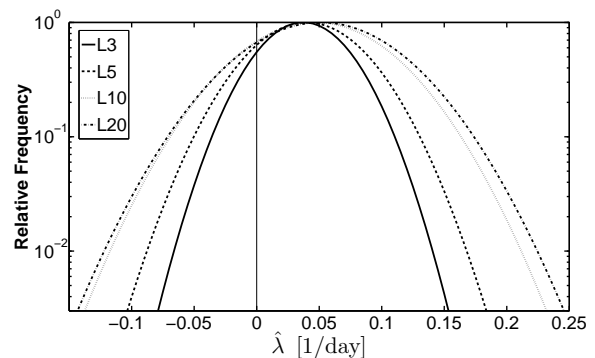


Figure 3. Gaussian fits of the local largest Lyapunov exponent distribution in T21 with different vertical levels L as indicated.

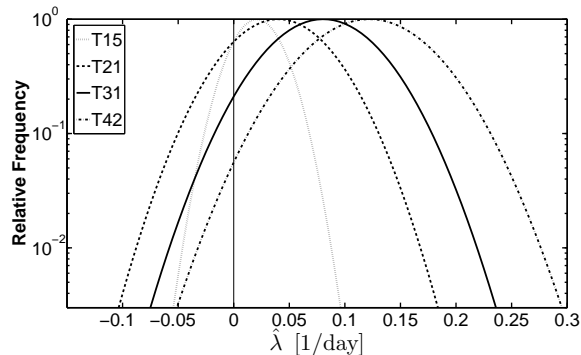


Figure 4. Gaussian fits of the local largest Lyapunov exponent distribution for $L = 5$ levels and different horizontal resolution, as indicated.

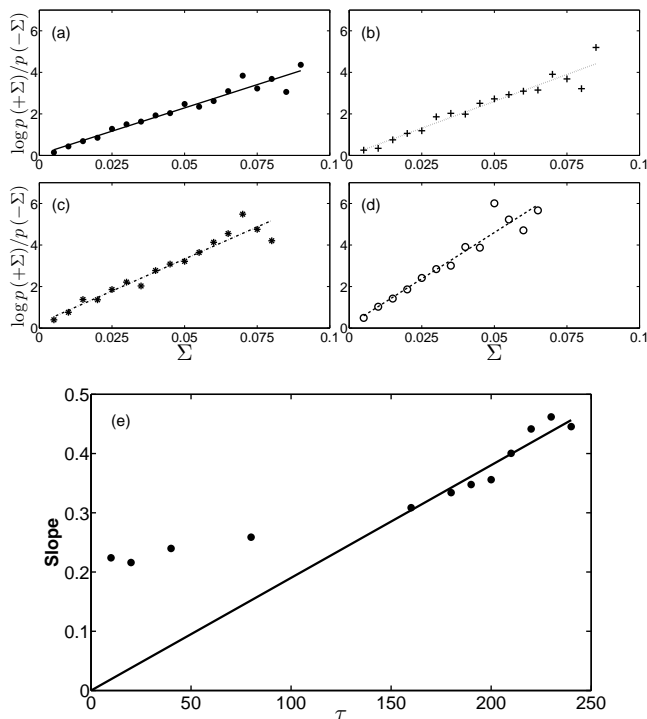


Figure 5. Logarithmic probability ratio of positive to negative entropy production rates for $\tau = 10\text{h}$ (a), $\tau = 80\text{h}$ (b), $\tau = 160\text{h}$ (c) and $\tau = 240\text{h}$ (d) in T21L5 resolution. The slopes of the logarithmic probability ratios against τ (e).

V. SUMMARY AND CONCLUSIONS

The dynamic atmospheric model PUMA (Portable University Model of the Atmosphere) is used to assess the variability of predictability. The model has variable

vertical and horizontal resolutions and is used here for $L = 3$ to 20 levels and $\ell = 15$ to 42 spherical wave numbers. The model describes a standard dynamical core with diabatic heating and friction. In contrast to complex models, forcing and dissipation in PUMA are implemented as linear relaxation processes. This keeps the system simple to concentrate on the effects of the non-linear dynamics.

The local (time-dependent) largest Lyapunov exponent $\hat{\lambda}$ is estimated by the divergence of two close 200 years trajectories, a reference and a perturbation; the latter being rescaled in regular time intervals. The distances between both trajectories are measured by a Euclidean metric comprising all dynamic variables at all grid points.

The main interest is in the frequency of negative $\hat{\lambda}$ which is associated with increased predictability (return of skill) and negative entropy production. Note that in contrast to the analysis of [18] where a regional analysis is presented, the results in the present paper correspond to the global circulation.

For moderate resolutions below $\ell = 42$ wave numbers the distribution of $\hat{\lambda}$ shows a considerable ratio of negative values (up to 20%), hence negative entropy production and violation of the second law of thermodynamics. This effect is negligible for $\ell \geq 42$.

The increase of vertical and horizontal resolution shows different effects: The vertical resolution mainly increases the variance of the $\hat{\lambda}$ distribution while the horizontal resolution primarily increases the mean. These results suggest a method to determine an optimal combination of horizontal wave numbers and vertical levels in numerical models. The widening of the distributions for increasing vertical resolutions enhances fluctuations and can lead to an increased frequency of circulation extremes.

This study demonstrates the validity of the fluctuation theorem in an atmospheric model with the entropy production rate approximated by the local largest Lyapunov exponent.

The resolutions used here are standard in many global warming scenarios and even lower resolutions are used for long term integrations. The results show that numerical models used in geophysical fluid dynamics may be considered as mesoscopic systems.

ACKNOWLEDGMENTS

We like to thank Edilbert Kirk and Davide Faranda for helpful discussions. BS acknowledges funding by the cluster of excellence Integrated Climate System Analysis and Prediction (CliSAP, University of Hamburg). KF acknowledges support by a Max-Planck Fellowship.

[1] D. J. Evans, E. G. D. Cohen, and G. P. Morriss, Phys. Rev. Lett. **71**, 2401 (1993)

[2] G. Gallavotti and E. G. D. Cohen, Physical Review Letters **74**, 2694 (1995)

- [3] S. Ciliberto and C. Laroche, *Le Journal de Physique IV* **08**, 5 (1998)
- [4] G. Gallavotti, L. Rondoni, and E. Segre, *Physica D: Non-linear Phenomena* **187**, 338 (2004)
- [5] J. L. Anderson and H. M. van den Dool, *Mon. Wea. Rev.* **122**, 507 (1994)
- [6] P. B. Rhines, *J. Fluid Mech.* **69**, 417 (1975)
- [7] M. Casartelli, E. Diana, L. Galgani, and A. Scotti, *Phys. Rev. A* **13**, 1921 (1976)
- [8] G. Benettin, L. Galgani, and J.-M. Strelcyn, *Phys. Rev. A* **14**, 2338 (1976)
- [9] L.-S. Young, *Entropy* (Princeton University Press, 2003) Chap. 16
- [10] H. Fujisaka, *Progress of Theoretical Physics* **70**, 1264 (1983)
- [11] T. Yoshida and S. Miyazaki, *Progress of Theoretical Physics Supplement* **99**, 64 (1989)
- [12] K. Fraedrich, E. Kirk, U. Luksch, and F. Lunkeit, *Meteorol. Zeitschrift* **14**, 735 (2005)
- [13] K. Fraedrich, *Eur. Phys. J. Plus* **127**, 53 (2012)
- [14] S. A. Orszag, *J. Atmos. Sci.* **27**, 890 (1970)
- [15] J. Harlim, M. Oczkowski, J. A. Yorke, E. Kalnay, and B. R. Hunt, *Phys. Rev. Lett.* **94**, 228501 (2005)
- [16] L. A. Smith, C. Ziehmann, and K. Fraedrich, *Quart. J. Roy. Meteorol. Soc.* **125**, 2855 (1999)
- [17] J. P. Peixoto and A. H. Oort, *Physics of climate* (AIP, New York, 1992)
- [18] D. J. Patil, B. R. Hunt, E. Kalnay, J. A. Yorke, and E. Ott, *Phys. Rev. Lett.* **86**, 5878 (2001)